

Effect of Gamma Irradiation on the Structure, Optical and Thermal Properties of PC–PBT/NiO Polymer Nanocomposites Films

S. A. Nauh^{1,2} · B. O. Alsobhi¹ · A. Abou Elfadl^{3,4} · A. M. Massoud^{2,5}

Received: 8 June 2017 / Accepted: 14 August 2017 / Published online: 18 August 2017
© Springer Science+Business Media, LLC 2017

Abstract Bayfol (PC–PBT blend-film) is a class of polymeric solid state nuclear track detector which has a lot of applications in several radiation detection fields. It is a bisphenol-A polycarbonate PC blended with polybutylene terephthalate PBT. Bayfol/nickel oxide (PC–PBT/NiO) nanocomposite films have been deposited using molding technique. It is worth mentioning that this report is almost the first one dealing with the topic of the changes of physical properties of Bayfol/NiO nanocomposite due to gamma irradiation. Samples from PC–PBT/NiO (5 w%) nanocomposite were irradiated with gamma doses in the range 20–250 kGy. The structural modifications in the gamma irradiated nanocomposite samples have been studied as a function of dose using different characterization techniques such as X-ray diffraction, UV spectroscopy, color difference studies, differential scanning calorimetry and scanning electron microscope. The results indicate the proper dispersion of NiO nanoparticles in the PC–PBT matrix that causes a strong intermolecular interaction between NiO and PC–PBT, resulted in an increase in refractive index and the amorphous

phase. Also, it is found that the gamma irradiation reduces the optical energy gap that could be attributed to the increase in structural disorder of the irradiated PC–PBT/NiO nanocomposites due to crosslinking. Further, the color intensity ΔE , which is the color difference between the non irradiated sample and the irradiated ones, was greatly increased with increasing the gamma dose, conveyed by a significant increase in the red and yellow color components.

Keywords Nanocomposites · XRD · UV spectroscopy · Color · DSC · SEM

1 Introduction

Polycarbonates (PC) are used in many applications because of their distinguished properties as excellent toughness, high rigidity, and good heat resistance. Also, it has a low resistance to organic compounds [1]. On the other hand, polybutylene terephthalate PBT possess a very high resistance to organic chemicals because they are semi-crystalline. These materials are also stiff, and can be hold up to high temperatures. The crystallinity of PBT leads them to be of high specific gravity as well as high shrinkage values [2]. Bayfol is a polymeric solid state nuclear track detector that has benefits over standard polycarbonate films. It is a thermoplastic alloy of amorphous polycarbonate and semi-crystalline polybutylene terephthalate (PC–PBT) [3]. Blends of polycarbonate and polybutylene terephthalate PBT are an important class of commercial blends with numerous applications providing good chemical resistance, impact resistance even at low temperatures, and improved flow characteristics as compared with the neat polymers [4]. Devaux et al. [4] have postulated transesterification to be the most important exchange reaction occurring between PC and PBT, resulting in a new

✉ S. A. Nauh
samin273@gmail.com

¹ Physics Department, Faculty of Science, Taibah University, Medina, Saudi Arabia

² Physics Department, Faculty of Science, Ain Shams University, Cairo, Egypt

³ Physics Department, Preparatory Year, Deanship of Educational Services, Taibah University, Medina, Saudi Arabia

⁴ Physics Department, Faculty of Science, Fayoum University, Fayoum, Egypt

⁵ Physics Department, Faculty of Science, Jazan University, Jizan, Saudi Arabia

chemical structure of copolymers. In the current research, the properties of our PC/PBT alloys are enhanced by adding nanoparticles during compounding. Nickel oxide (NiO) nanoparticles (NPs) have exceptional properties compared to its bulk such that it can be used in industrial products supporting new applications [5]. Nanocomposites are a relatively new class of materials with ultrafine phase dimensions (few nanometers) [6]. The merging of metal nanoparticles in the PC matrix will improve its physical properties so that the obtained nanocomposite will be suitable for different applications such as biotechnology, packaging, microelectronics, energy storage, optical devices and food-stabilizing systems [7–9]. On the other hand, the irradiation of polymer films can persuade several changes in both optical and structural properties [10]. Molecular chain scission, intermolecular crosslinking, formation of C=C, and carbon-rich clusters are some of the structural deformations in the irradiated polymer which modify the physical properties of the material [1, 3]. The prompted photo-chemical properties change in polymer films have been grabbed attention for numerous applications, such as optical memories, switching devices, holographic image recording and waveguide lithography [11]. Quanaxiao et al. [12], studied the effect of addition of MgO nanoparticle to PC. It was found that the particle with the size of 200 nm is the nanoparticle that has the potential to enhance the diffusion within PC matrix and produce composite with uniform properties. Also, Vividha et al. [13], investigated the structure and optical properties of ZnO/polycarbonate nanocomposite. They observed that the nanocomposite films have potential in many packaging applications because of their effective antibacterial and UV-blocking properties and hydrophobic nature. Several studies have been performed on the modification of the physical properties of polymers using nanoparticles [14–24]. The present study deals with the investigation of gamma irradiation on the structure and optical properties of PC–PBT/NiO nanocomposites, aiming to study the possibility of enhancing their properties and refining their performance in different applications.

2 Experimental

2.1 Samples

2.1.1 Preparation of NiO Nanoparticles

NiO nanoparticles were prepared by sol gel route. The materials used to synthesize the nanoparticles contain nickel nitrate hexahydrate ($\text{Ni}(\text{NO}_3)_2 \cdot 6\text{H}_2\text{O}$), ethylene glycol ($\text{C}_2\text{H}_6\text{O}_2$) and Citric acid ($\text{C}_6\text{H}_8\text{O}_7 \cdot \text{H}_2\text{O}$), purchased from Sigma-Aldrich GmbH, Cairo, Egypt. Deionized water were used as a solvent. To obtain the gel, a certain amount of nickel nitrate hexahydrate (1 mol), citric acid (3 mol) and 0.5 ml of ethylene glycol

were dissolved in a beaker containing 50 ml of the solvent deionized water. To ensure solution homogeneity, the solution was continuously stirred for 24 h at room temperature. Then the solution was left to dry. After drying, the final resulting product was annealed at a temperature of 800 °C for 1 h to remove all the remaining organic compounds, finally cooled to room temperature. The sample was investigated by XRD. MAUD software [25] and Popa anisotropic model [26] were used to refine the crystal structure of NiO nanoparticles. The powder morphology was verified by transmission electron microscope (TEM, JEOL JEM-100CX) with accelerating voltage up to 100 kV.

2.1.2 Preparation of PC/NiO Nanocomposites

Nanocomposite films of PC–PBT/NiO with 5 wt% NiO prepared by casting technique. Bayfol CR 1–4 is a bisphenol-A polycarbonate with a chemical composition of $\text{C}_{16}\text{H}_{14}\text{O}_3$ blended with polybutylene terephthalate PBT. It is developed by Farbenfabriken Bayer A.G., Leverkusen, Germany, with an average thickness of 250 μm and density 1.20 g/cm^3 . Bayfol was dissolved in methylene chloride at room temperature using a magnetic stirrer. The synthesized NiO nanoparticles were added with 5 wt% to the PC–PBT solution, under magnetic stirring, according to the following equation:

$$x(\text{wt}\%) = \frac{w_f}{w_p + w_f} \times 100 \quad (1)$$

where w_f and w_p represent the weight of NiO and PC–PBT, respectively. Finally, the aqueous mixture was casted into cleaned Petri dishes and placed in closed box for 3 days. The obtained nanocomposite films with about 100 μm thickness were then characterized. The thickness was measured by a thickness gauge Model 11/2704 Ast MD 370 standard which was calibrated by Arab British Dynamics [1].

2.2 Irradiation Facilities

The irradiation was carried out with ^{60}Co Gamma source (manufactured by Atomic Energy of Canada Ltd.) with energies in the order of 1.173 and 1.332 MeV, at a dose rate of 2.4 Gy/min at NCRRT, Atomic Energy Authority, Cairo, Egypt. The samples were irradiated at different absorbed doses 20, 50, 100, 150, 200 and 250 kGy, at the same condition. The dose was adjusted by the Far West Technology FWT'60-00 dosimeter that was calibrated by the CERIC/CEROUS dosimeter, supplied by Nordion, Canada.

2.3 Analysis of the Nanocomposite Samples

A Shimadzu 6000 X-ray diffractometer identified with Cu- k_{α} radiation of wavelength $\lambda = 1.5406 \text{ \AA}$ was used to perform X-ray diffraction (XRD) patterns.

UV/Vis spectroscopy measurements were conducted by UV/Vis Spectrophotometer (Model Tomos UV-1800) in the wavelength range from 1100 to 190 nm, in transmission mode, using thin solid film of synthesized quantum composites. The Commission International de E' Claire (CIE units x, y and z) methodology was applied in this work for the description of colored samples. The tristimulus values and the CIELAB color difference were calculated using the methodology described before [27].

The thermal behavior was investigated using differential scanning calorimetry (DSC) with a type Setaram labsys TG-DSC16 instrument. $\alpha\text{-Al}_2\text{O}_3$ powder was used as a reference for DSC measurements. Thermal experiments were carried out on all samples at a heating rate of 10 C/min with Ar as a carrier gas at a flow rate of 30 cm^3/min .

The nature and morphology of PC-PBT/NiO nanocomposites were studied by a scanning electron microscope SEM Model JCM 6000, JEOL Company.

3 Results and Discussion

3.1 X ray diffraction XRD

Rietveld refinement of XRD pattern of NiO using MAUD program is shown in Fig. 1a. As illustrated in our previous work [4], the refinement confirmed that the sample is single phase with space group (R-3m). The value of the crystallite size, obtained from Rietveld structure refinement for NiO sample is 18 nm. Figure 1b shows the TEM images for NiO sample. The particles generally have a spherical shape and tend to agglomerate due to their mutual interactions.

X-ray diffraction measurements were carried out on the non-irradiated and irradiated PC-PBT/NiO nanocomposites in the 2θ range $10\text{--}80^\circ$ (Fig. 2). The X-ray diffraction patterns of the samples are characterized by halos extending in the 2θ range $13^\circ\text{--}28^\circ$ with maximum diffraction intensity observed at 2θ values ranging from 18° to 22° . The X ray diffraction pattern of the non irradiated PC-PBT/NiO nanocomposite indicates the semi-crystalline nature of the synthesized polymer with a dominant amorphous phase. The diffraction patterns of the samples irradiated in the dose range 20–200 kGy show the competition between degradation (chain scission) and crosslinking processes until finally the degradation predominates at 200 kGy. This degradation can reduce the number of entanglements per molecule. Chain scission can also act to reduce intermolecular stress in the amorphous region, thus increasing chain mobility. The

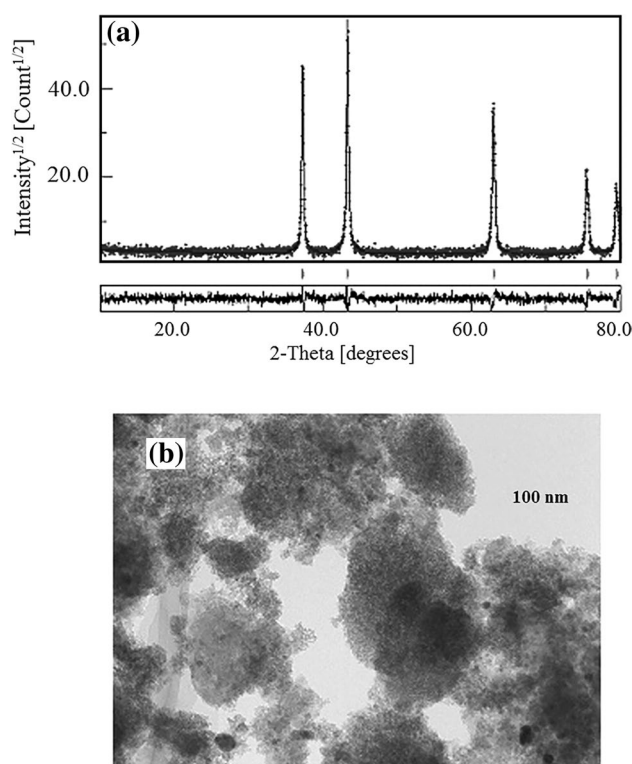


Fig. 1 a Rietveld refinement profile for NiO sample obtained from MAUD software, b SEM micrographs of NiO nanoparticles films

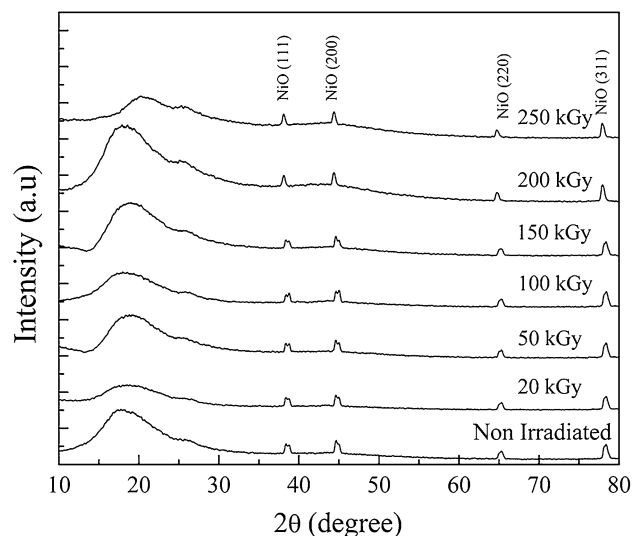


Fig. 2 The X-ray diffraction patterns of the non-irradiated and irradiated PC-PBT/NiO nanocomposites films

increase in mobility allows some molecules to reordered. Increasing the gamma dose above 200 and up to 250 kGy is reflected in a decrease in the integral intensity, area under the halo (Fig. 2), indicating that the ordering structure has

been destroyed. This could be attributed to the crosslinking that changes the previously regularly arranged portions into nonarranged ones by forming new bonds between NiO and the PC–PBT chains. Besides, the synthesis of PC–PBT requires transesterification of diphenyl carbonate with bisphenol A with the elimination of phenol as side product. Therefore, it is expected that the initial concentration of the hydroxyl group will monotonously decrease with an increase in the chain length of the polymer [1]. The spectra of all samples were fitted with a Lorentz function. Thereby the values of integral intensity I (area) of the main diffraction peak were extracted and are given in Table 1.

Since the halo's width at the half of maximal intensity ΔW is inversely proportional to the crystallite size L according to the Scherrer equation:

$$L = \frac{K\lambda}{(\Delta W \cos \theta)} \quad (2)$$

where λ (1.54 nm) is the wavelength of the Cu- K_{α} X-ray radiation used, θ is the Bragg angle (in radians), k the Scherrer constant (≈ 1), values of ΔW were calculated. Table 1 shows the variation of ΔW with the gamma dose. From the figure it is seen that ΔW exhibited a non monotonic trend with the gamma dose.

3.2 Optical Analysis

PC–PBT/NiO nanocomposite films have been characterized through spectral absorption measurements. The UV–Vis absorption spectra of the irradiated and non-irradiated PC–PBT/NiO nanocomposite films are shown in Fig. 3. As seen, the absorbance changes with changing dose up to 250 kGy. This means that the levels at the energy band were affected by the gamma doses and the Rayleigh scattering from the embedded NiO nanoparticles [28, 29].

Table 1 Values of integral intensity I and the width at half maximal intensity Δw as a function of 2θ and gamma dose

Gamma dose (kGy)	2θ	I (counts)	Δw (radian)
0	18.76	7922	0.280
20	19.12	4835	0.338
50	19.63	5753	0.246
100	19.01	6104	0.304
150	19.75	7168	0.247
200	19.18	10,483	0.268
250	21.63	6843	0.376

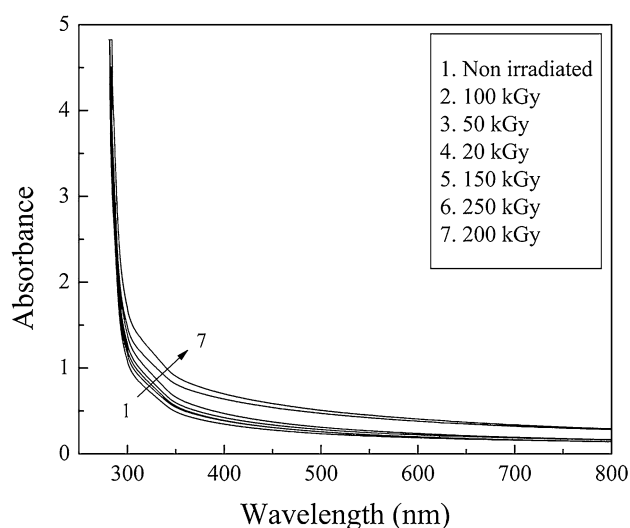


Fig. 3 The UV–Vis absorption spectra of the non-irradiated and irradiated PC–PBT/NiO nanocomposites films

In amorphous, disordered and defected materials, there are tail states appear in gap region below the fundamental absorption edge [30] which can be determined using the absorption coefficient (α). This absorption coefficient (α) obeys the Urbach rule [31]:

$$\alpha = \alpha_o \exp\left(\frac{h\nu}{E_u}\right) \quad (3)$$

where α_o is a constant that characterize the materials and E_U is the Urbach energy that refers to the width of the tail states. Plotting the relation between $\ln \alpha$ and $h\nu$ for the irradiated and non irradiated PC–PBT/NiO nanocomposite films, the E_U could be obtained from the reciprocal of the slope of the straight line. The values of E_U were found to increase with increasing the gamma dose (Fig. 4), this means that the NiO

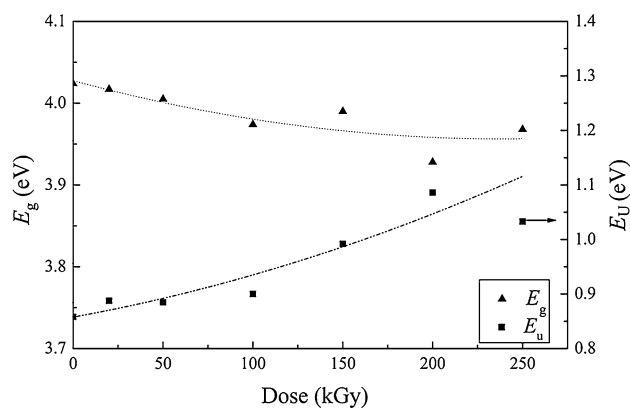


Fig. 4 Variation of Urbach's energy and the energy band gap with the gamma dose

creates defects in PC–PBT [32]. The energy band gap (E_g) is determined using the UV/Vis absorption spectra using Tauc's relation [33]:

$$\alpha h\nu = B(h\nu - E_g)^n \quad (4)$$

where α is the absorption coefficient, $h\nu$ is the incident photon energy that can be approximated to $h\nu = 1240/\lambda$, B is a constant and n assumes to be $ne = 1/2$ and $3/2$ for direct allowed and forbidden transitions, respectively, $n = 2$ and 3 for indirect allowed and forbidden transitions, respectively. The variation of optical band gap with the gamma dose is shown in Fig. 4. It is clear that the energy gap decreases with increasing the dose up to 250 kGy. This indicates that the gamma irradiation affect the nanocomposite to crosslink. This crosslinking is caused by the formation of new covalent bonds between NiO and PC–PBT and therefore new different chains were obtained, in turn hindered the motion of molecules and reduce their activity and consequently decrease the optical band gap [34, 35].

The refractive index of optical materials is very important for many electronic and optoelectronic applications. The refractive index of the nanocomposite samples is calculated using the following Eq. (5) and is plotted in Fig. 5, at different wavelengths, versus gamma dose.

$$n = \left(\frac{1+R}{1-R} \right) + \sqrt{\frac{4R}{(1-R)^2} - K^2} \quad (5)$$

where n is the real part of the complex refractive index. $RR = 1 - \sqrt{Te^A}$ is the reflection, which has been calculated from the absorbance spectra. T is the transmittance and k is the extinction coefficient calculated from the equation:

$$k = (\alpha/4\pi) \quad (6)$$

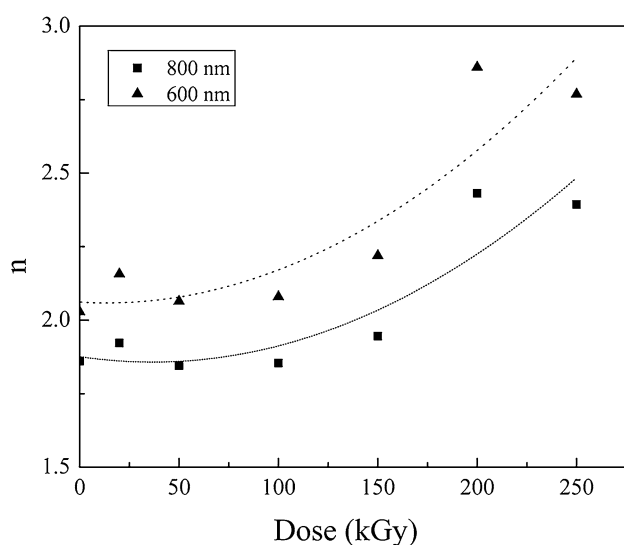


Fig. 5 Variation of refractive index with the gamma dose

where α is the absorption coefficient which can expressed by

$$\alpha = \frac{\text{Absorbance}}{\text{Sample thickness}} \quad (7)$$

It is clear from Fig. 5 that the refractive index increases with increasing the dose. Moreover, in visible optical region, the refractive index of the irradiated PC–PBT/NiO nanocomposites is enhanced than the non-irradiated one. This means that the gamma irradiation enhances the spread of NiO inside the PC matrix. This helps in the formation of intermolecular hydrogen bonding between NiO with the adjacent OH group of PC, and in turn minimizes the anisotropic character of the nanocomposite samples [3].

3.3 Color Changes

The vision scientists created a special set of mathematical lights, X, Y and Z, to replace actual red, green and blue lights. Every color can be matched using the appropriate amount of X, Y and Z light. The amounts of X, Y and Z light needed to match a color are called the color's tristimulus values [36]. Using the transmission data of the non-irradiated and irradiated PC–PBT/NiO nanocomposites in the wavelength range of 370–780 nm, represented in Fig. 6, both the tristimulus values and chromaticity coordinates were analyzed. Figure 7 shows the variation of tristimulus values (X, Y, Z) with the gamma dose. From the figure, X, Y and Z exhibited the same trend, where they almost decreased on increasing the dose up to 250 kGy. Figure 8 shows the variation of chromaticity coordinates

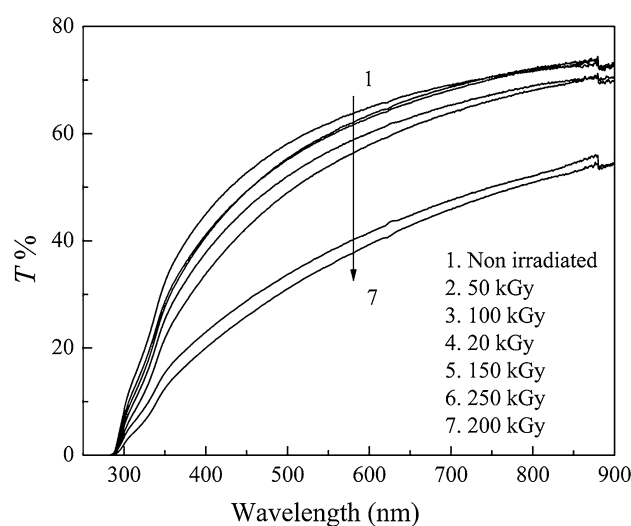


Fig. 6 The UV–Vis transmission spectra of the non-irradiated and irradiated PC–PBT/NiO nanocomposites films

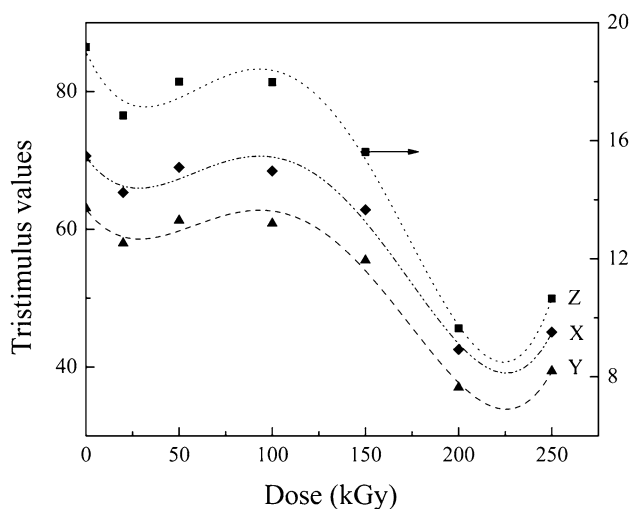


Fig. 7 Variation of tristimulus values (X, Y, Z) with the gamma dose

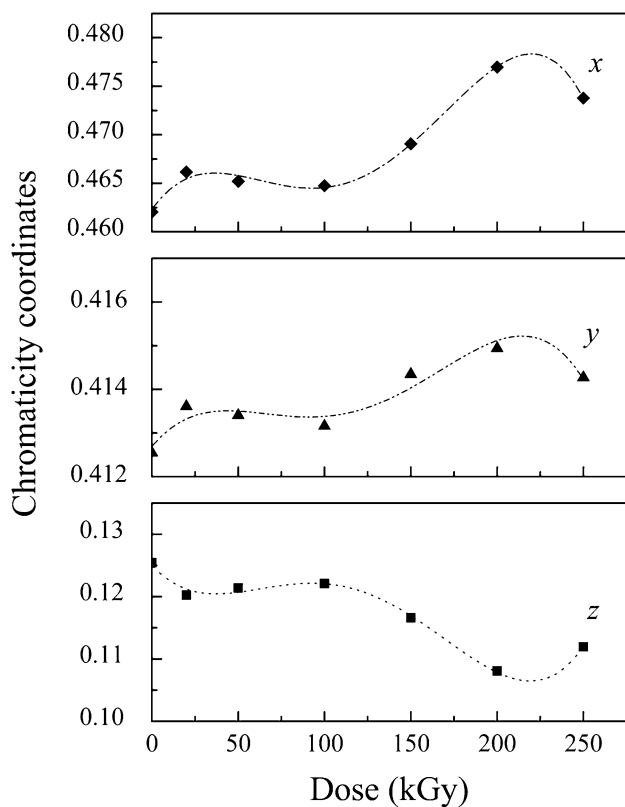


Fig. 8 Variation of chromaticity coordinates (x, y, z) with the gamma dose

(x, y, and z) with the gamma dose. It is seen that x and y exhibited the same trend, where they showed an increase with increasing the dose up to 250 kGy. The chromaticity coordinate z exhibited an opposite trend. The variation of

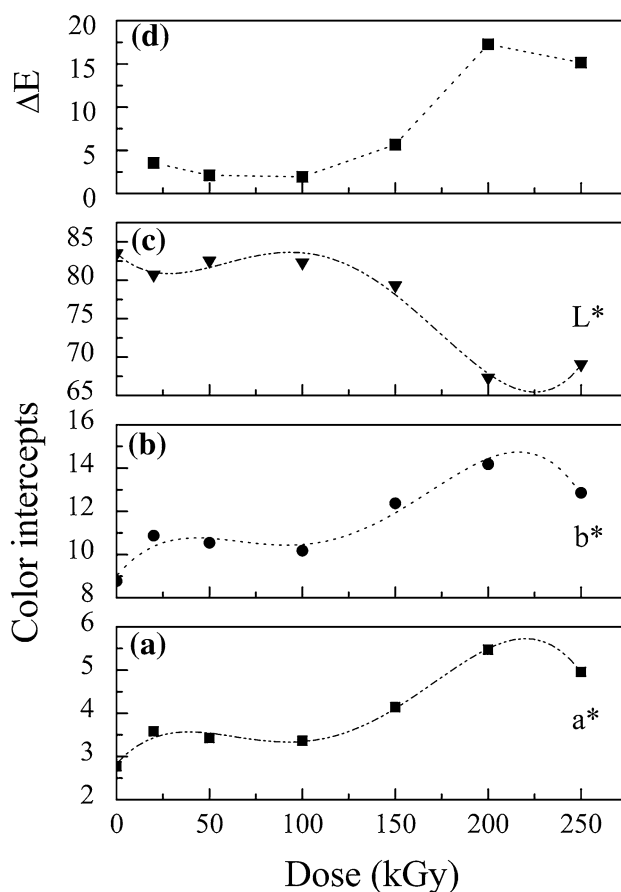


Fig. 9 Variation of the color intercepts (L^* , a^* and b^*) and the color intensity ΔE with the gamma dose

the color intercepts (a^* , b^* and L^*) with the gamma dose is shown in Fig. 9. It could be noted that the L^* intercepts of zero and 100 integers represent the standard dark and white colors, respectively. The positive values of a^* and b^* represent the red and yellow components, whereas the negative values represent the green and blue color components, respectively [37]. The accuracy in measuring L^* is ± 0.05 , and is ± 0.01 for a^* and b^* . It can be seen that the color parameters a^* , b^* and L^* were significantly changed after exposure to gamma irradiation. The green color component ($-a^*$) is changed into red ($+a^*$) (Fig. 9a). At the same time, the blue ($-b^*$) color component of the blank film is changed into yellow ($+b^*$) (Fig. 9b) after exposure to gamma dose up to 250 kGy. This was accompanied by a net increase in the darkness of the samples ($-L^*$) (Fig. 9c).

The color intensity ΔE , which is the color difference between the blank and irradiated samples could be calculated using the CIELAB color difference Eq. [27] and is plotted in Fig. 9d as a function of dose. The color intensity ΔE shows an increase with increasing the gamma dose in the dose range 100–250 kGy. The changes in color could be

attributed to the variation of microstructure and trapping of the excited free radicals that are formed by ionization. In addition, the trapped free radicals resulting from radiation-induced break of polymer molecules have electrons with unpaired spin, which may give optical coloration [27]. Comparing these results with those obtained before for the response of Bayfol polymer to color changes under irradiation [3, 38] we find that the trend of the red–green color component of the non irradiated Bayfol sample is affected by the addition of NiO nanoparticles and thus contributing to the color changes, whereas it was not affected by the irradiation before.

3.4 Differential Scanning Calorimetry (DSC)

DSC is a technique used to study the thermal transitions and the changes that take place in polymers when they are heated. DSC was performed in the temperature range from room temperature up to 300 °C at a heating rate 10 °C/min, on irradiated and non-irradiated nanocomposites. The obtained thermograms are given in Fig. 10a. From the figure, it is observed that all the thermograms are characterized by the appearance of one endothermic peak due to glass transition temperature T_g . The values of T_g

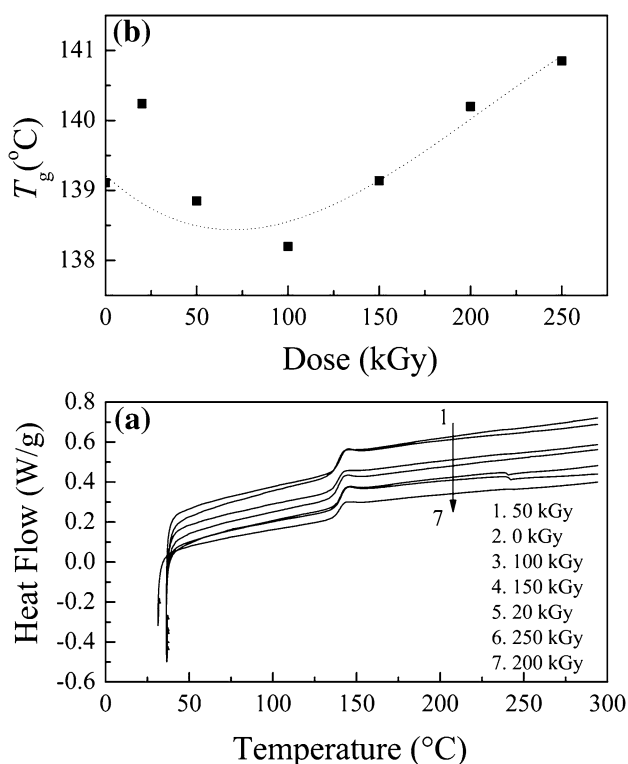


Fig. 10 a DSC thermograms for the non-irradiated and irradiated PC-PBT/NiO nanocomposites, b Variation of the glass transition temperature with the gamma dose

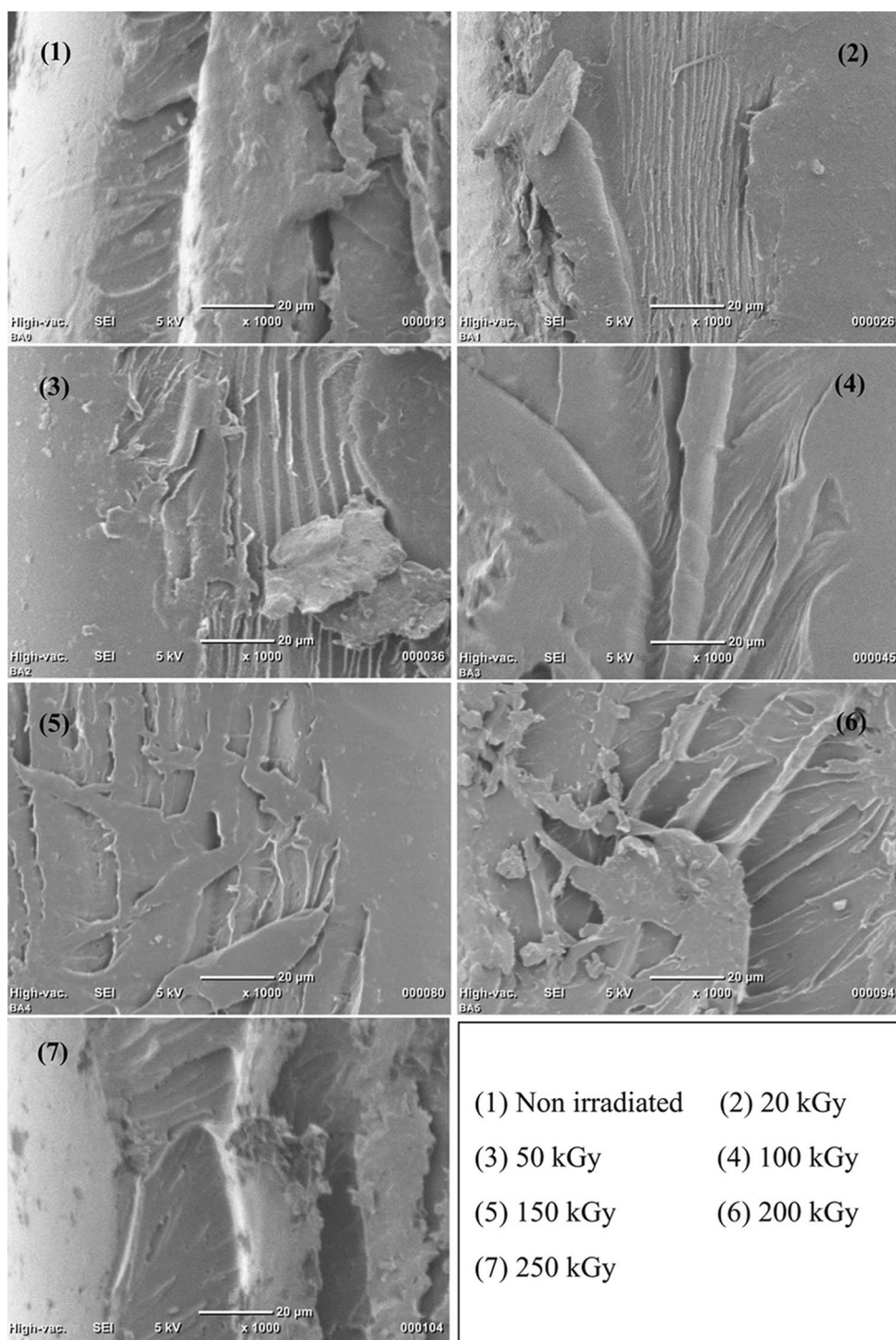
were evaluated and plotted as a function of gamma dose in Fig. 10b. As can be seen from the figure, T_g decreases gradually with increasing dose up to 100 kGy as a consequence of chain scission which occurs readily within the amorphous region. On increasing the dose up to 250 kGy, T_g increases. The increase in T_g could be regarded to the crosslinking which is possible during chain scission, and inhibits crystallization of the nanocomposites.

It is obvious that the trend exhibited by T_g is similar to that obtained by refractive index. This trend can be explained on the basis that the irradiation causes chain scission and thus the molecules become shorter. These shorter chains are less entangled and have better mobility, thus allowing re-orientation of the molecules. The re-orientation of the molecules results in the formation of a crystalline phase. However, the crystalline region formed consists of chains that are more oriented and closely packed as compared to the amorphous region. The proximity of the polymer chains in the crystalline structure encourages the trapped free radicals to recombine, thus reducing the number of effective chain scission. This effect is also known as the “cage effect”, a concept which involves the recombination of free radicals before they can diffuse out of the active region and undergo reactions that encourage crosslinking. Besides, it is known that the $-\text{CH}_3$ groups in polycarbonate produce a steric hindrance which weakens the bonds of the backbone of the chain [39]. This weakness is annihilated by the intermolecular hydrogen bonding between NiO with the OH group of PC.

3.5 Scanning Electron Microscope (SEM)

The SEM micrographs of the non-irradiated and irradiated PC-PBT/NiO nanocomposites are shown in Fig. 11. The set of photos (from 1 to 7), which deals with the same sample zone, has been taken by increasing the gamma dose, i.e. 0, 20, 50, 100, 150, 200 and 250 kGy. It is seen that all the samples contain fibers. Each fiber is composed of a bunch of fibrils. The fibrils as shown in Fig. 11 seem to be oriented along with the fibers’ axis and their sizes are found to be increasing with increasing the gamma doses. This orientation is attributed to the effective interfacial adhesion between the NiO nanoparticles and the polymer chains. Moreover, the monomer molecules are uniformly polymerized on the surface of NiO oxide nanoparticles and thereby attain regularity in the polymer matrix [40]. To fully understand the morphological structures of the nanocomposites, higher magnification ($\times 2000$) SEM images for the non irradiated and some irradiated PC-PBT/NiO nanocomposite samples have been provided in Fig. 12.

Fig. 11 SEM micrographs of the non-irradiated and irradiated PC–PBT/NiO nanocomposites (The set of photos from 1 to 7 corresponds to the gamma doses 0, 20, 50, 100, 150, 200 and 250 kGy, respectively)

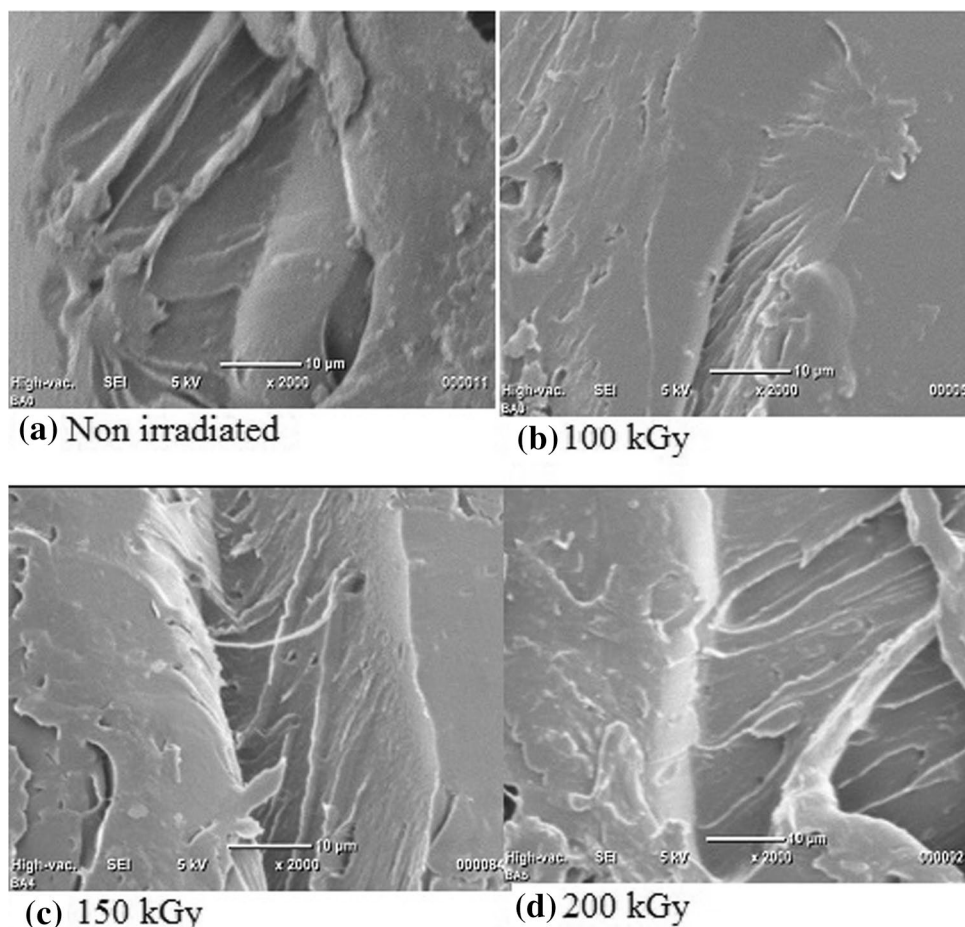


4 Conclusion

Prolonged gamma irradiation up to 250 kGy changes the regularly arranged portions into non-arranged ones by forming new bonds between NiO and the PC–PBT chains through crosslinking. This enhances the resilience of the PC–PBT/

NiO polymer. Also, the refractive index calculations confirm that the gamma irradiation leads to the predominance of the crosslinking, and in turn minimizes the anisotropic character of the nanocomposite samples. In addition, the results of optical properties reveal that the gamma irradiation up to 250 kGy reduces the optical energy gap that could be

Fig. 12 SEM micrographs of the non-irradiated and some irradiated PC–PBT/NiO nanocomposites with higher magnification ($\times 2000$)



attributed to the increase in structural disorder of the irradiated PC–PBT/NiO nanocomposites due to crosslinking. This allows the formation of color centers with a significant increase in the red and yellow color components that establish color differences between the non-irradiated sample and those irradiated with different doses.

References

1. S.A. Nouh, A. AbouElfadl, K. Benthame, *Radiat. Eff. Def. Solids* **172**, 48–60 (2017)
2. S.A. Nouh, H.A. El-Nabarawy, M.M. Abutalib, R.A. Bahareth, *Eur. Phys. J. Appl. Phys.* **62**, 1–5 (2013)
3. S.A. Nouh, Y.E. Radwan, D. El fiky, M.M. Abutalib, R.A. Bahareth, T.M. Hegazy, S.S. Fouad, *Radiat. Phys. Chem* **97**, 68–74 (2014)
4. J. Devaux, P. Godard, J.P. Mercier, *J. Polym. Sci. Polym. Phys Edn.* **20**, 1895–1900 (1982)
5. S.A. Nouh, K. Benthame, A. AbouElfadl, *Radiat. Eff. Def. Solids* **171**, 1016–1027 (2016)
6. S.A. Nouh, M.J. Tommalieh, N.T. El-Shamy, *Radiat. Eff. Def. Solids* **170**, 548–555 (2015)
7. P.C. Rishi, M. Suman, A.K. Tomar, K. Shyam, *J. Alloys Compd.* **538**, 212–219 (2012)
8. M. Akbarzadeh, H. Ebaidehaghani, M. Sadeghi, *Adv. Mater. Res.* **739**, 51–56 (2013)
9. Z.A. Nimrodh, S. Umopathy, *Appl. Nano Sci.* **1**, 87–96 (2011)
10. M.D. Megahed, H.M. Zidan, *Curr. Appl. Phys.* **6**, 91–96 (2006)
11. S. Xie, A. Natansohn, P. Rochon, *Chem. Mater.* **5**, 403–411 (1993)
12. D. Quanxiao, G. Chong, D. Yanfen, W. Feng, W. Bin, Z. Shimin, W. Tongxin, Y. Mingshu, *J. Appl. Polym. Sci.* **123**, 1085–1093 (2012)
13. D. Vividha, G. Namrata, V.M. Priyesh, B. Shaibal, V.D. Vishwas, K. Shivajirao, K. Pawan, *Nanocomposites* **1**, 106–112 (2015)
14. B.R.K. Blackman, H. Steininger, J.G. Williams, K. Zuo, *Compos. Sci. Technol.* **122**, 10–17 (2016)
15. D.R. Son, A.V. Raghu, K.R. Reddy, H.M. Jeong, *J. Macromol. Sci. Part B* **55**, 1099–1110 (2016)
16. S.J. Han, H. Lee, H.M. Jeong, B.K. Kim, A.V. Raghu, K.R. Reddy, *J. Macromol. Sci. Part B* **53**, 1193–1204 (2014)
17. K.R. Reddy, M. Hassan, V.G. Gomes, *Appl. Catal. A* **489**, 1–16 (2015)
18. K.R. Reddy, K.V. Karthik, S.B. Prasad, S.K. Soni, H.M. Jeong, A.V. Raghu, *Polyhedron* **120**, 169–174 (2016)
19. M. Cakici, K.R. Reddy, F.A. Marroquin, *Chem. Eng. J.* **309**, 151–158 (2017)
20. M.U. Khan, K.R. Reddy, T. Snguanwongchai, E. Haque, V.G. Gome, *Colloid. Polym. Sci.* **294**, 1599–1610 (2016)
21. Y. Hanifehpour, N. Hamnabard, B. Mirtamizdoust, S.W. Joo, *J. Inorg. Organomet. Polym.* **26**, 623–631 (2016)

22. B. Mirtamizdoust, *Ultrason. Sonochem.* **35**, 263–269 (2017)
23. B. Mirtamizdoust, D.C. Bienko, Y. Hanifehpour, E.R.T. Tiekink, V.T. Yilmaz, P. Talemi, S.W. Joo, *J. Inorg. Organomet. Polym.* **26**, 819–828 (2016)
24. Y. Hanifehpour, A. Morsali, B. Soltani, B. Mirtamizdoust, S.W. Joo, *Ultrason. Sonochem.* **34**, 519–524 (2017)
25. L. Lutterotti, *J. Appl. Cryst.* **2**, 33–35 (2000)
26. N.C. Popa, *J. Appl. Cryst.* **31**, 176–180 (1998)
27. S.A. Nouh, M. Amal, R.A. Bahareth, M.M. Abutalib, K. Benthami, *Eur. Phys. J. Appl. Phys.* **65**, 1–5 (2014)
28. B.S. Rathore, M.S. Gaur, K.S. Singh, *J. Appl. Polym. Sci.* **126**, 960–968 (2012)
29. S. Ilican, Y. Caglar, M. Caglar, F. Yakuphanoglu, *Phys. E* **35**, 131–138 (2006)
30. A.E. Rakhshani, *J. Phys.* **12**, 4391–4400 (2000)
31. F. Urbach, *Phys. Rev.* **92**, 1324–1324 (1953)
32. P.C. Rishi, M. Suman, A.K. Tomar, S. Kumar, *Digest J. Nanomater. Biostructures* **6**, 299–303 (2011)
33. J. Tauc, in *Optical Properties of Solids*, ed. by F. Abeles (North-Holland Publications, Amsterdam, 1972), p. 77
34. H.A. Yasser, A. Amr, F. Ghada, M.R. Reda, *World J. Condens. Matter Phys.* **1**, 12–18 (2011)
35. E. Sayeda, E. Seif, M. Nehad, *Open J. Polym. Chem.* **4**, 21–30 (2014)
36. K. Nassau in *Color for Science, Art and Technology* (Elsevier, New York, 1998)
37. H.M. Said, Z.I. Ali, H.E. Ali, *J. Appl. Polym. Sci* **101**, 4358–4365 (2006)
38. S.A. Nouh, S. Bahmmam, *Radiat. Eff. Def. Solids* **167**, 102–110 (2012)
39. S.A. Nouh, N.I. El-Tayeb, A.F. Said, M.M. Radwan, S.A. EL-Fiki, *Radiat. Meas.* **42**, 8–13 (2007)
40. M.T. Ramesan, V. Nidhisha, P. Jayakrishnan, *Polym. Int.* **66**, 548–556 (2017)